Supporting Information

Ultrahigh Energy Storage Performances of Polymer-based Nanocomposite via Interfaces Engneering

Peng Wang[a, d], Zhongbin Pan[a, b]*, Weilin Wang[a], Jianxu Hu[a], Jinjun Liu[a], Jinhong Yu[e], Jiwei Zhai[d], Qingguo Chi [b]*, and Zhonghui Shen[c]*

[a]School of Materials Science and Chemical Engineering, Ningbo University, Zhejiang, Ningbo 315211, China. Email: panzhongbin@163.com (Zhongbin Pan)

[b]Key Laboratory of Engineering Dielectrics and Its Application, Ministry of Education, Harbin University of Science and Technology, Harbin, 150080, China. Email: qgchi@hrbust.edu.cn (Qingguo Chi)

[c]State Key Laboratory of Advanced Technology for Materials Synthesis and Processing, Center of Smart Materials and Devices, Wuhan University of Technology, Hubei, Wuhan 430070, China. E-mail: zhshen@whut.edu.cn (Zhonghui Shen)

[d]School of Materials Science & Engineering, Tongji University, 4800 Caoan Road, Shanghai 201804, China.

[e]Key Laboratory of Marine Materials and Related Technologies, Zhejiang Key Laboratory of Marine Materials and Protective Technologies, Ningbo Institute of Materials, Technology and Engineering, Chinese Academy of Sciences, Zhejiang, Ningbo 315201, China.

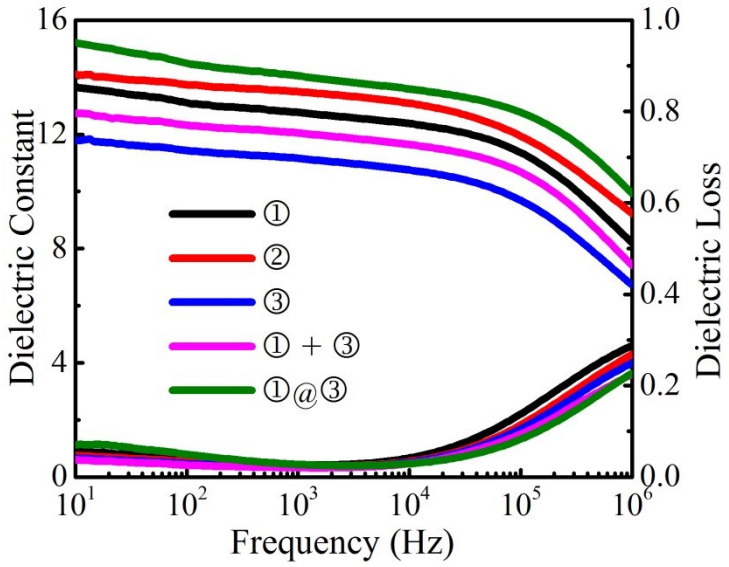

Figure S1. Dielectric constant and dielectric loss as function of frequency of nanocomposites films with 3 vol.% different structure of nanofillers.

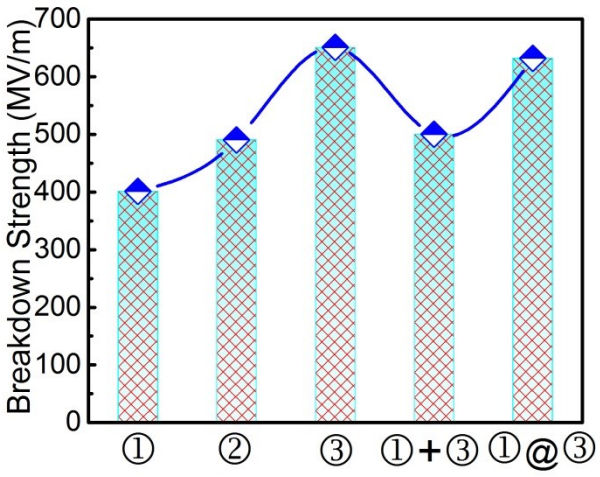

Figure S2. Breakdown strength of nanocomposites films with 3 vol.% different structure of nanofillers.

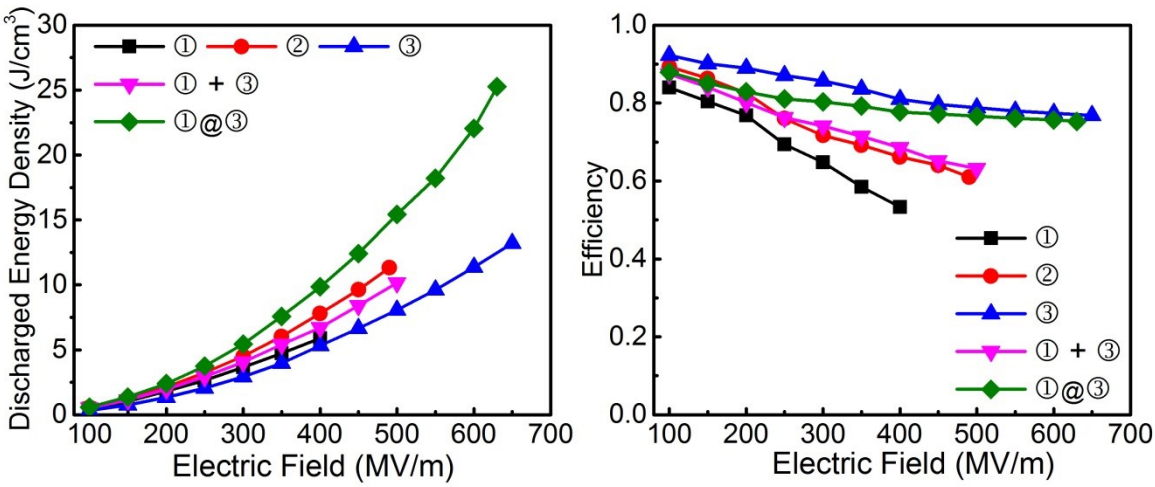

Figure S3. a) Discharged energy density and b) efficiency of nanocomposites films with 3 vol.% different structure of nanofillers.

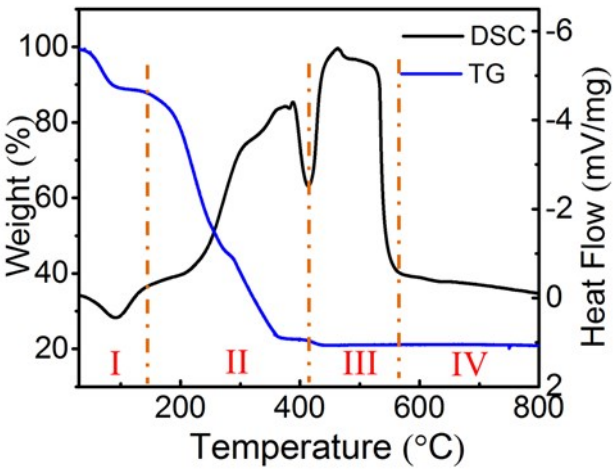

Figure S4. TG-DSC curves of the as-electrospun composite nanofibers.

Based on the DSC curve, the total weight loss occurs at three stages in the formation process. As shown in Figure 3, the TG curves have the first weight loss at period I, which may be caused by the evaporation of residual water and solvent. Also an exothermic effect appears on the DSC curve. An intensive exothermal peak is found at 95 °C, which can be ascribed to a loss of non-structural water molecules. The sharp weight loss at period II could be seen. One possible reason is that the organic functional groups in the raw materials were destroyed, which was accompanied by an exothermal peak on the DSC curve. At the period III and IV, with temperatures rise, the weight loss is not found, suggesting that the pure $SrTiO_3$ have formed.

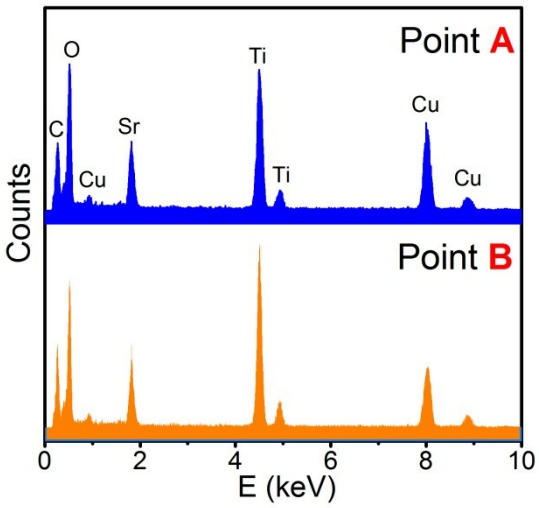

Figure S5. EDS of the ST@ST NFs with point A and point B.

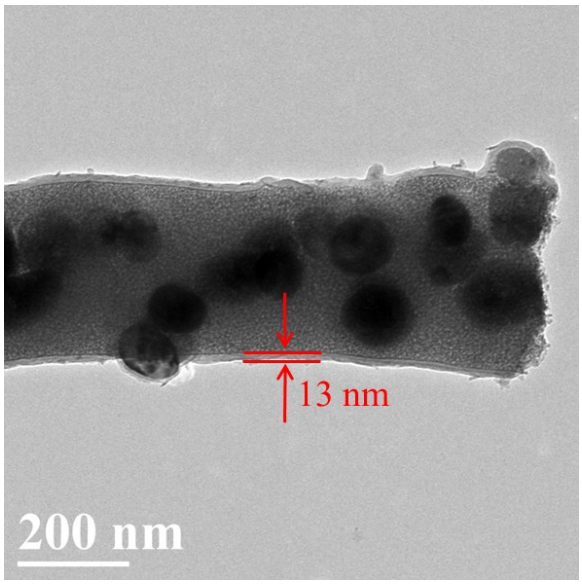

Figure S6. TEM images of dopamine modification of ST@ST NFs.

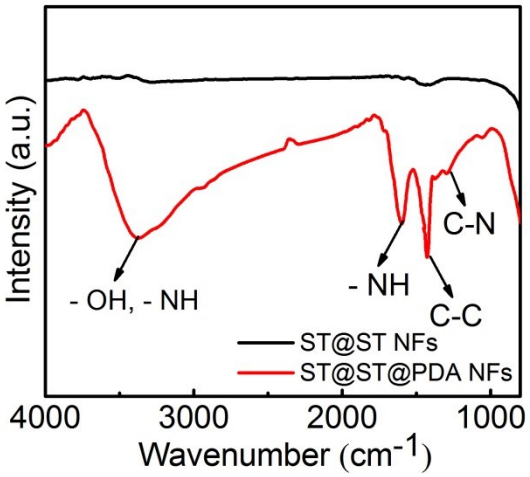

Figure S7 FT-IR of dopamine modified and un-modified of ST@ST NFs.

As compare with the unmodified of ST@ST NFs, surface modification with dopamine of ST@ST NFs are new characteristic absorbance peaks, which are 3100-3700 cm^{-1}, 1626 cm^{-1}, 1505 cm^{-1}, and 1254 cm^{-1}, corresponding to -NH and/or -OH stretching vibrations, -NH bending vibration, -C-C stretching vibration, and -C-N stretching vibration, respectively.

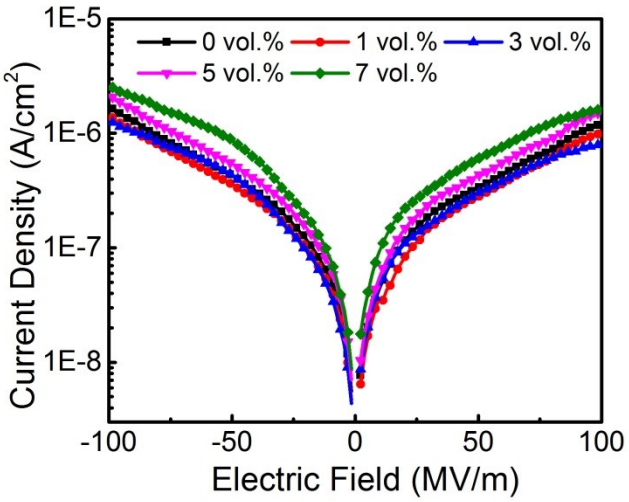

Figure S8. Leakage current density of pristine P(VDF-HFP) and a series of ST@ST NFs/PVDF-HFP nanocomposite films

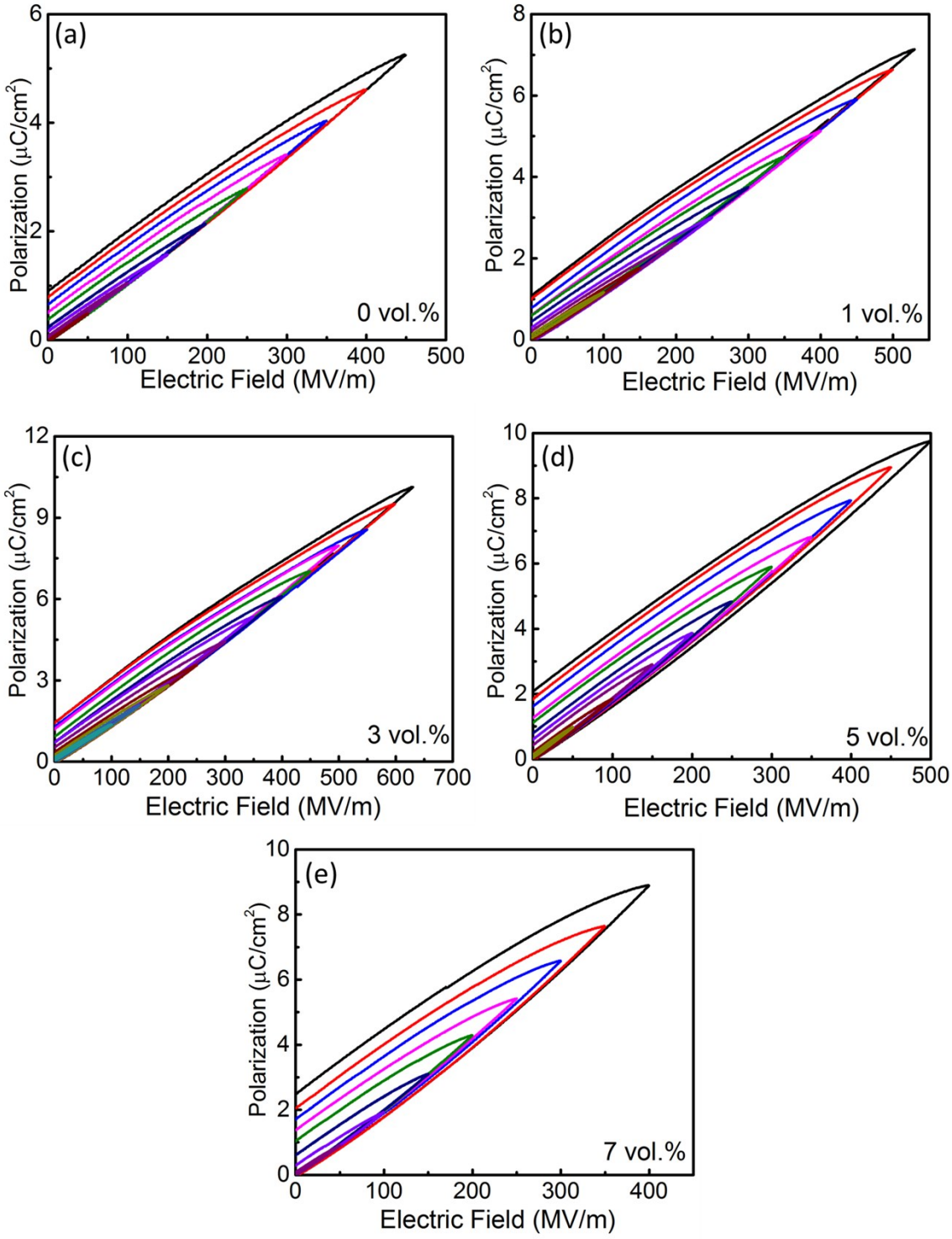

Figure S9. D-E loops of pristine P(VDF-HFP) and a series of ST@ST NFs/PVDF-HFP nanocomposite films: a) 0 vol.%, b) 1 vol.%, c) 3 vol.%, d) 5 vol.% and e) 7 vol.%.

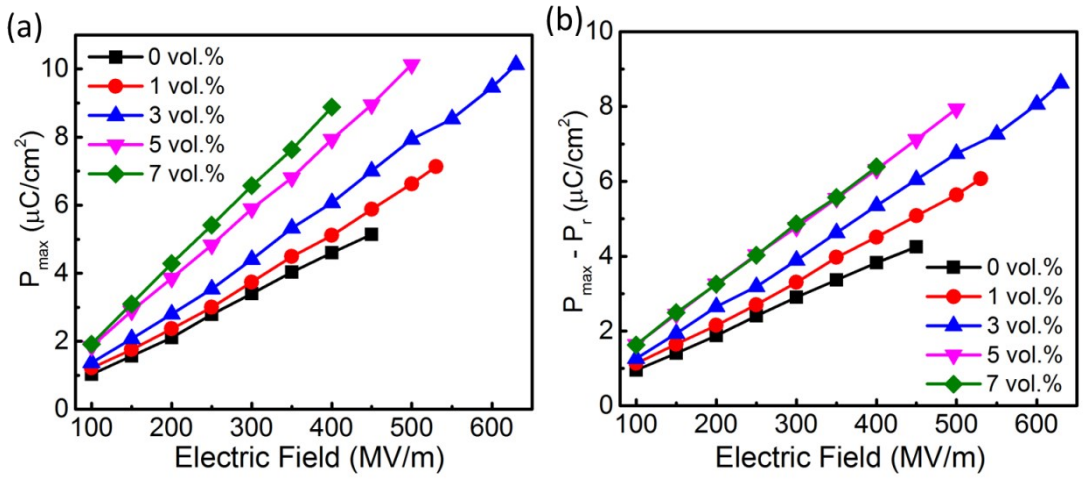

Figure S10. a) P_{max} and b) $P_{max} - P_r$ of pristine P(VDF-HFP) and a series of ST@ST NFs/PVDF-HFP nanocomposite films.